Study of the Secondary Structure of the C-Terminal Domain of the Antiapoptotic Protein Bcl-2 and Its Interaction with Model Membranes[†,‡]

María del Mar Martínez-Senac, Senena Corbalán-García, and Juan C. Gómez-Fernández*

Departamento de Bioquímica y Biología Molecular A, Facultad de Veterinaria, Universidad de Murcia, Apartado de Correos 4021, E-30080 Murcia, Spain

Received February 3, 2000; Revised Manuscript Received April 21, 2000

ABSTRACT: Bcl-2 is a protein which inhibits programmed cell death. It is associated to many cell membranes such as mitochondrial outer membrane, endoplasmic reticulum, and nuclear envelope, apparently through a C-terminal hydrophobic domain. We have used infrared spectroscopy to study the secondary structure of a synthetic peptide (a 23mer) with the same sequence as this C-terminal domain (residues 217−239) of Bcl-2. The spectrum of this peptide in D_2O buffer shows an amide I′ band with a maximum at 1622 cm^{-1}, which clearly indicates its tendency to aggregate in aqueous solvent. However, the peptide incorporated in multilamellar phosphatidylcholine membranes shows a totally different spectrum of the amide I′ band, with a maximum at 1655 cm^{-1}, indicating a predominantly α-helical structure. Addition of the peptide to unilamellar vesicles destabilized them and released encapsulated carboxyfluorescein. Differential scanning calorimetry of dimyristoylphosphatidylcholine multilamellar vesicles in which the peptide was incorporated revealed that increasing concentrations of the peptide progressively broadened the pretransition and the main transition, as is to be expected for a membrane integral molecule. Fluorescence polarization of 1,6-diphenyl-1,3,5-hexatriene in fluid phosphatidylcholine vesicles showed that increasing concentrations of the peptide produced increased polarization values, pointing to an increase in the apparent order of the membrane and indicating that high concentrations of the peptide considerably broaden the phase transition of dimyristoylphosphatidylcholine multilamellar vesicles. Quenching the intrinsic fluorescence of the Tyr-235 of the peptide, by KI, indicated that this aminoacyl residue is highly exposed to aqueous solvent when incorporated in phospholipid vesicles. The results are discussed in terms of their relevance to the proposed topology of insertion of Bcl-2 into biological membranes.

Apoptosis is a physiological process involving programmed cell death. It is regulated by a number of genes which encode proteins which either activate or inhibit this process. Bcl-2 is a potent inhibitor of apoptotic cell death, the *bcl-2* gene being discovered because of its involvement in the t(14:18) chromosomal translocations commonly found in lymphomas (*1*). Although many proteins are known to be involved in the control of apoptosis, the Bcl-2 family of proteins is thought to be central regulators (*2*, *3*). In vertebrates, several Bcl-2 homologues have been identified, some of which function as inhibitors (Bcl-x_L, Mcl-1, and A1) and others as promoters of cell death (Bcl-x_S, Bax, Bak, and BAD). These Bcl-2 family members are characterized by their ability to interact and form homo- and heterodimers (*4*). The balance in the contents of the anti- and proapoptotic Bcl-2 homologues determines the sensitivity of cells to apoptotic signals (*2*, *5*), although the mechanisms by which Bcl-2 inhibits apoptosis remain to be fully elucidated.

It has been proposed that Bcl-2 and some of the proteins which form part of its family may inhibit cell death in many ways, although they can be classified into two different groups. One of the pathways increases mitochondrial membrane permeability, possibly by the insertion in the membrane of helices α5 and α6 (*6*−*13*), which modulate the release of cytochrome *c* from mitochondria to the cytosol (*14*−*16*), interfere with the production of free radicals, translocate granzyme to the nucleus (*17*), and regulate intracellular calcium homeostasis, because of their channel-forming ability (for reviews see refs *18*−*20*). In the other pathway Bcl-2 binds to and possibly modulates the function of a number of proteins which are important for apoptosis, such as R-Ras (*21*), Raf-1 (*22*), calcineurin (*23*), the p53-binding protein 53BP2 (*24*), or the p53 (*25*).

Although Bcl-2 and its homologues have been observed to form membrane channels by using helices α5 and α6, Bcl-2 also has a C-terminal hydrophobic stretch, which has been proposed to be inserted into the membrane, thus targeting it to intracellular membranes, such as the outer membrane of mitochondria, the nuclei, and the endoplasmic reticulum membranes (*26*−*29*). The presence of the hydrophobic C-terminal tail has been described as improving protective effects, such as cell survival after IL-3 deprivation (*30*) and the suppression of apoptosis caused by E1B-defective adenovirus (*31*). Nevertheless, this C-terminal hydrophobic domain does not seem to be essential for other antiapoptotic functions because it can be substituted by other

[†] This work was supported by Grants PB95-1022 and PB98-0389 from Dirección General de Enseñanza Superior e Investigación Científica, Madrid, Spain.

[‡] This paper is dedicated to the memory of the late Prof. Dennis Chapman FRS.

* To whom correspondence should be addressed. Telephone: 34-968364766. Fax: 34-968364147. E-mail: jcgomez@fcu.um.es.

10.1021/bi000256h CCC: $19.00
Published on Web 06/08/2000

hydrophobic domains which are known to act as hydrophobic anchors for other proteins (*32*, *33*).

Bcl-2 protein and other proteins of this family have been cloned and expressed for study at high resolution. However, most of these studies used truncated forms which do not include the C-terminal hydrophobic domain of Bcl-2 protein (*12*, *33*−*35*). The same is true for other proteins of the same family such as Bax (*35*−*37*) and even with the high-resolution structures obtained for Bcl-x_L (*38*, *39*). The reason for this is that the soluble protein which results from the elimination of the highly hydrophobic C-terminal domain can be produced in the high quantities required for structural studies, whereas full proteins are hardly produced. As a consequence, nothing has been experimentally learned about the structure of the C-terminal domain.

In the present study we obtained a synthetic peptide (23mer) with the same sequence as the 217−239 C-terminal part of Bcl-2 and studied its secondary structure by infrared spectroscopy and its interaction with model membranes. We demonstrate that it may insert in the membrane in a predominantly α-helical structure, confirmation of which is its capacity to disturb the physical properties of the phospholipid bilayer as seen through the release of encapsulated carboxyfluorescein and by biophysical techniques, such as differential scanning calorimetry and fluorescence polarization of the membrane probe DPH.[1]

EXPERIMENTAL PROCEDURES

Materials. The synthetic peptide encompassing residues 217−239 of Bcl-2 ($^{+}$HN-^{217}LKTLLSLALVGACITLGAY-LGHK^{239}-COO^{-}) was obtained from Genemed (San Francisco, CA) and judged pure (>95%) according to HPLC and MALDITOF spectroscopy. Egg yolk phosphatidylcholine (EYPC) and dimyristoylphosphatidylcholine (DMPC) were obtained from Avanti Polar Lipids (Alabaster, AL). D_2O and TFE were purchased from Sigma Chemical Co. (Madrid, Spain), and all other solvents were from Merck (Darmstadt, Germany). All other reagents used were of analytical grade.

Secondary Structure Prediction. The PredictProtein Service (http://www.embl-heidelberg.de/predictprotein/predictprotein.html) at EMBL (Heidelberg, Germany) was used following the Rost and Sander method (*40*, *41*).

Infrared Spectroscopy. The infrared measurements were performed on a Philips PU9800 Fourier transform infrared spectrometer equipped with a deuterated triglycine sulfate detector. Each spectrum was obtained by collecting 128 interferograms with a nominal resolution of 2 cm^{-1} and triangular apodization using the sample shuttle accessory in order to average background spectra between sample spectra over the same time period. The spectrometer was continuously purged with dry air. Samples were prepared from EYPC or Bcl-2 C-terminal domain stocks dissolved in chloroform/methanol (1:1 v/v). The Bcl-2 C-terminal domain (0.115 μmol) alone or with phospholipid (1.15 μmol) was dried under a stream of N_2, free of O_2, and the last traces of solvents were removed by a further 3 h evaporation under high vacuum. Then, 200 μL of TFE was added, and the solution was vortexed vigorously, dried under a stream of nitrogen, and stored under vacuum for 3 h to remove the organic solvent totally. Samples were then hydrated in 25 μL of D_2O buffer (10 mM Hepes, 0.1 mM EDTA, pD 7.4) and dispersed with vigorous vortex mixing in the liquid-crystalline phase to form multilamellar vesicles (MLV) in the case of the sample containing phospholipid. Samples were then transferred to a Specac 20710 cell equipped with CaF_2 windows and 25-μm Teflon spacers (Specac, Kent, U.K.). Spectral subtraction was performed interactively using the Spectra-Calc program (Galactic Industries Corp., Salem, NH). Data treatment and band decomposition of the original amide I′ have been described previously (*42*, *43*). The position of individual band was obtained from the resolution-enhanced spectrum. The fractional areas of bands in the amide I′ region were calculated from the final fitted band areas.

To check if the peptide was incorporated into the liposomes, the hydrated mixture was centrifuged at 13200*g* for 30 min, to sediment the multilamellar liposomes, and the peptide was searched in both supernatant and pellet by SDS−PAGE as described (*44*). Using this qualitative procedure no peptide was detected in the supernatant whereas a great amount of it was present in the pellet, thus indicating that the peptide was massively incorporated into the liposome membranes.

Quenching by Iodide. Iodide quenching experiments were carried out essentially as described (*45*). Samples were prepared by mixing EYPC and peptide in chloroform/methanol (1:1 v/v) or peptide alone. They were then prepared as described above for infrared spectroscopy experiments. Each assay mixture contained 15 μg of Bcl-2 C-terminal domain peptide and EYPC at a peptide/lipid molar ratio of 0.022 or 15 μg of peptide alone, in 1.8 mL of 0.1 mM EDTA, 10 mM Hepes, pH 7.4, and 0−0.5 M KI. Ionic strength was adjusted by addition of KCl. KI solutions contained 10^{-4} M $S_2O_3^{2-}$ to prevent I_3^- formation (*45*).

Tyrosine fluorescence emission was monitored using a Shimadzu RF-540 spectrofluorophotometer with excitation at 295 nm (10-nm slit width) and emission intensity was from 300 to 400 nm (10-nm slit width). Measurements were performed in a thermostated 2.5 mL and 1 cm path-length quartz cuvette at room temperature (25 °C). The inner filter effect was corrected as described (*45*).

Quenching kinetic parameters were calculated from a modified Stern−Volmer equation (*45*)

$$\frac{F_0}{\Delta F} = \frac{1}{f_a K_Q [Q]} + \frac{1}{f_a'}$$

where F_0 is the fluorescence intensity in the absence of the quencher (Q), ΔF is the change in fluorescence intensity due to the addition of a given concentration of Q, K_Q is a quenching constant which is the product of the collisional quenching rate constant and fluorescence lifetime in the absence of the quencher, and f_a' is the effective fraction of the tyrosyl fluorescence that is quenchable.

Fluorescence Polarization. The fluorescent probe 1,6-diphenyl-1,3,5-hexatriene (DPH) was prepared in tetrahy-

[1] Abbreviations: CF, 5(6)-carboxyfluorescein; CL, cardiolipin; DMPC, dimyristoylphosphatidylcholine; DPH, 1,6-diphenyl-1,3,5-hexatriene; DSC, differential scanning calorimetry; EYPC, egg yolk phosphatidylcholine; MLV, multilamellar vesicles; PC, phosphatidylcholine; PE, phosphatidylethanolamine; PI, phosphatidylinositol; PG, phosphatidylglycerol; SUV, small unilamellar vesicles; TFE, 2,2,2-trifluoroethanol.

drofuran, and its concentration was determined by UV spectroscopy using an absorption coefficient of 88 000 M^{-1} cm^{-1} at 452 nm in methanol.

Multilamellar vesicles of DMPC or EYPC were prepared with adequate amounts of peptide and phospholipids of the respective stock solutions in chloroform/methanol (1:1) to give the different peptide/lipid molar ratios studied. DPH was added to the organic solvent solution, before drying, to give a probe/lipid molar ratio of 1:500.

DPH fluorescence polarization was measured in a Shimadzu RF-540 spectrofluorophotometer equipped with a polarization accessory. Excitation and emission wavelengths were 350 and 452 nm, respectively, with an excitation and emission slit width of 5 nm. Cuvette temperature was monitored continuously by means of a thermistor probe. Fluorescence polarization was measured as a function of temperature from 9 to 50 °C. Measurements were performed every 2 °C. A small magnetic stirring bar in the cuvette prevented settling of the vesicles.

In the fluorescence polarization experiment, the sample was excited with a polarized beam, and the components of the emission parallel or perpendicular to the direction of the excitation beam were measured. The polarization of the emitted fluorescence, *P*, was determined as

$$P = \frac{1 - (I_{90,0}/I_{90,90})(I_{0,90}/I_{0,0})}{1 + (I_{90,0}/I_{90,90})(I_{0,90}/I_{0,0})}$$

where a correction factor for the instrumental response of the two components of the emission has been applied (*46*). $I_{90,0}$ is the fluorescence intensity when the excitation polarizer is perpendicular to the direction of the beam and the emission is parallel; $I_{90,90}$ and $I_{0,0}$, when perpendicular and parallel, respectively, and $I_{0,90}$, when the excitation polarizer is parallel and the emission polarizer is perpendicular to the direction of the beam.

To ensure that there was no polarization due to light scattering, polarization was measured before and after sample dilution. In cases when dilution led to an increased level of *P*, the samples were diluted until the value of *P* remained constant.

Differential Scanning Calorimetry. Calorimetric measurements were performed in a Microcal MC-2 differential scanning calorimeter (Microcal Inc., Northampton, MA). All heating scans were recorded at the same rate of 60 °C/min in the temperature interval from 5 to 40 °C. Before each scan was begun, the samples were equilibrated in the calorimetric cell for 15 min at 5 °C. Appropriate amounts of peptide and 1 mg of DMPC of the respective stock solutions in chloroform/methanol (1:1 v/v) were dried under a stream of N_2, free of O_2, and the last traces of solvents were removed by a further 3 h evaporation under high vacuum. Then, 200 μL of TFE was added, and the solution was vigorously vortexed, dried under a stream of nitrogen, and stored in vacuo for 3 h to remove the organic solvent totally. The samples were then dispersed in a 135 mM NaCl, 10 mM Hepes, pH 7.4, buffer, hydrated in the liquid-crystalline phase with vigorous vortex mixing to form MLV. Finally, a reference containing buffer and sample was placed into the calorimetric cells for the measurement, and the results were plotted as a function of the peptide/lipid molar ratios. The exact lipid concentration was determined according to the method of Böttcher et al. (*47*). The main transition peaks corresponding to some thermograms were decomposed by using Spectra-Calc software (Galactic Industries Corp., Salem, NH) through Datafit. The best fit was to two components. ΔH values, onset temperatures, and half-bandwidths were obtained according to the ORIGIN software package supplied by Microcal (Microcal Inc., Northampton, MA).

Leakage of Liposome Contents. The leakage of liposome contents to the external medium was kinetically monitored by measuring the release of the 5(6)-carboxyfluorescein (CF) trapped inside the vesicles (*48*−*51*). The fluorescent dye CF was obtained from Kodak (Eastman Kodak Co.) and contained hydrophobic impurities. Purification of this commercial dye was carried out by gel filtration on a Sephadex LH-20 (Pharmacia) (1 × 30) column. An aqueous solution of 200 mM CF was prepared in 10 mM Hepes, pH 7.4. The concentration of CF was determined by ultraviolet spectroscopy using an absorption coefficient of 70 000 M^{-1} cm^{-1} at 493 nm. The dye solution was stored at 4 °C in the dark.

Small unilamellar vesicles (SUV) were prepared from an EYPC stock dissolved in chloroform/methanol (1:1). A total of 6.25 mg of phospholipid was dried under a stream of N_2, free of O_2, and the last traces of solvents were removed by a further 3 h evaporation under high vacuum. Phospholipid was then hydrated in a 10 mM Hepes, pH 7.4, buffer containing 200 mM purified CF (*49*) and dispersed by vortexing. Lipid suspension was sonicated at 4 °C for 20 min under a nitrogen atmosphere, using a microtip sonicator. The resulting solution was centrifuged at 13 000 rpm for 20 min to remove titanium particles and residual multilamellar structures. SUV were passed over a Sephadex G-50 (1 × 20) column and eluted with a 10 mM Hepes, pH 7.4, buffer containing 135 mM NaCl, isoosmolar with the CF buffer. Vesicles were separated from larger particles and untrapped CF eluting in the void volume of the column. To obtain homogeneous preparation, only the top fractions of the SUV elution peak were collected and pooled. Phospholipid concentration was determined according to the method of Böttcher et al. (*47*). The encapsulated volume was found to be 1.13 L/mol of phospholipid.

Carboxyfluorescein at 200 mM inside the EYPC SUV is mostly self-quenched, but when released into the media, such as by detergent solubilization of the vesicles, the diluted CF fluoresces intensely. The increase in CF fluorescence was followed using a Shimadzu RF-540 spectrofluorophotometer with excitation at 490 nm (5-nm slit width), and emission intensity was monitored at 520 nm (10-nm slit width). Measurements were made in a thermostated 2.5 mL quartz cuvette with constant stirring at room temperature (25 °C). A small volume of vesicles was diluted into the buffer (135 mM NaCl, 10 mM Hepes, pH 7.4) to yield a 2 mL total volume at a phospholipid final concentration of 6 μM. A baseline measurement of the fluorescence of vesicles alone was made for 10 min. In our experimental conditions, the spontaneous leakage rate was less than 3.5%. Then, the Bcl-2 C-terminal peptide, dissolved in TFE at 2 or 0.5 mg/mL, or TFE vehicle was added. Fluorescence was measured for 15 min, and then a small volume of concentrated Triton X-100 (0.5% final, w/v) was added in order to determine the maximum fluorescence attainable under conditions of totally solubilized vesicles. The addition of 3.4 μL of TFE did not produce any important leakage. The percentage of carboxy-

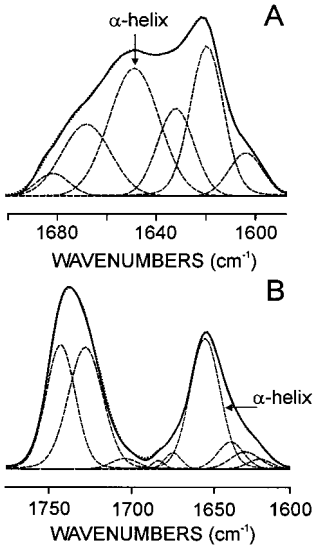

FIGURE 1: FT-IR spectrum of the Bcl-2 C-terminal domain in the absence (A) and in the presence (B) of multilamellar vesicles containing EYPC at a peptide/phospholipid molar ratio of 0.1 in D_2O buffer (solid line) with the fitted component bands (dashed line). The position of the individual band was obtained from the resolution-enhanced spectrum. The parameters corresponding to the component bands are reflected in Table 1. The dotted line represents the curve-fitted spectrum.

fluorescein released was determined by the equation $[(F_{t=15\ min} - F_0)/(F_{max} - F_0)] \times 100$, where $F_{t=15\ min}$ is the maximum intensity 15 min after addition of peptide or TFE, F_0 is the intensity of vesicles alone at time 0, and F_{max} is the intensity after addition of Triton X-100.

RESULTS

Secondary Structure of the Peptide As Studied by Infrared Spectroscopy. When the Bcl-2 C-terminal domain peptide was resuspended in D_2O buffer, in the absence of phospholipids, the amide I′ band of the infrared spectrum had its maximum at 1622 cm^{-1} (Figure 1A), a frequency which indicates the presence of aggregated peptide molecules with intra- or intermolecular hydrogen bonding and which is common usually in thermally denatured proteins (*53*−*56*). The amide I′ band was decomposed as shown in Figure 1A. The number and initial position of the component bands were obtained from band-narrowed spectra by Fourier deconvolution and derivation. The corresponding parameters, band position, percentage area, bandwidth of each spectral component, and assignment, are shown in Table 1. It can be seen that the spectrum exhibited six component bands in the 1700−1600 cm^{-1} region, and the quantitative contribution of each band to the total amide I′ contour was obtained by band curve fitting of the original spectrum. The component with the maximum contribution was located at 1649 cm^{-1}, which probably corresponds to α-helix, representing 35% of the total area. The assignment of α-helix to bands in the region 1648−1658 cm^{-1} is generally admitted (*57*, *58*). The component at 1623 cm^{-1} can be assigned to aggregated extended structures (*53*−*56*). The band at 1634 cm^{-1} can be attributed to β-sheets (*42*, *43*, *59*−*63*). The high-frequency components at 1668 and 1681 cm^{-1} can be assigned to turns (*64*−*68*).

The infrared spectrum was quite different when the Bcl-2 C-terminal domain was resuspended in the presence of multilamellar vesicles of EYPC; then the maximum of the amide I′ band was at 1655 cm^{-1}, indicative of a predominant α-helical structure (Figure 1B). The carbonyl ester band coming mainly from the phospholipid acyl chains may also be seen centered at 1737 cm^{-1} (Figure 1B). Band decomposition was made as in the sample of Figure 1A, and it can be seen that the main band was centered at 1656 cm^{-1}, indicating the predominance of an α-helical structure. The band at 1641 cm^{-1} can be assigned to unstructured conformations including open loops (*61*, *69*). The component at 1632 cm^{-1} can be attributed to intramolecular C═O vibrations of β-sheets (*42*, *43*, *59*−*63*). The high-frequency components at 1675 and 1684 cm^{-1} can be assigned to turns (*64*−*68*). Finally, the component at 1623 cm^{-1} is probably due to aggregated extended structures (*53*−*56*), as in the sample containing peptide without lipid, although in this case it is much smaller, representing only about 6% of the total area of the amide I′ band, indicating that most of the peptide aggregates have disappeared in the presence of the phospholipid. It should be also mentioned that the amide I′ band of the infrared spectrum of the peptide was not modified when phospholipid mixtures having a similar composition to liver mitochondrial membranes (*69*) were used instead of EYPC (data not shown for the shake of brevity). Concretely, the mixtures were PC/PE/PI/PG (45:30:18:7 molar ratio) (outer mitochondrial membranes) or PC/PE/PI/CL (49:30:11:11 molar ratio) (inner mitochondrial membranes). Note also that they included negatively charged phospholipids and PE (which does not favor a bilayer structure) but they did not modify the secondary structure of the peptide.

Table 1: FT-IR Parameters of the Amide I′ Band Components of the Bcl-2 C-terminal Domain in the Absence or Presence of Multilamellar Vesicles Containing EYPC in 10 mM Hepes and 0.1 mM EDTA−D_2O Buffer (pD 7.4)

peptide alone			peptide + EYPC		
position[a] (cm^{-1})	assignment	area[b] (%)	position[a] (cm^{-1})	assignment	area[b] (%)
1681	turns	4	1684	turns	2
1668	turns	19	1675	turns	5
1649	α-helix, random	35	1656	α-helix	68
1632	β-sheet	17	1641	random	12
1620	aggregation	28	1632	β-sheet	4
			1623	aggregation	4

[a] Peak position of the amide I′ band components. [b]Percentage area of the band components of amide I′. The areas corresponding to side chain contributions located at 1615−1600 cm^{-1} have not been considered.

The corresponding parameters, band position, percentage area, bandwidth, and assignment of each spectral component, are shown in Table 1. It is interesting that, according to the PredictProtein Service, using the Rost and Sander procedure (*40*, *41*), the peptide with the sequence corresponding to residues 217−239 of the C-terminal part of Bcl-2 should have a secondary structure with 87% α-helix and 13% loops, these nonhelical structures corresponding to aminoacyl residues located at both extremes of the peptide. This estimation correlates well with the experimental data obtained by infrared spectroscopy, in the presence of phospholipid, with the main component being α-helix, which amounts to 68% of the total structure.

Leakage of 6-Carboxyfluorescein Induced by Bcl-2 C-Terminal Domain Peptide. To further assess the insertion

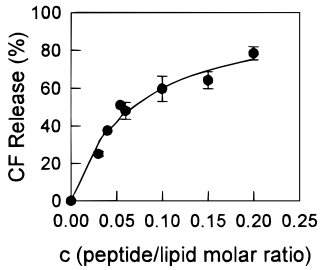

FIGURE 2: Leakage of carboxyfluorescein from EYPC (SUV) induced by the Bcl-2 C-terminal domain. The percentage of carboxyfluorescein released after 15 min of incubation with increasing concentrations of peptide was plotted as a function of the peptide/lipid molar ratio (c). 100% of leakage was established by lysing EYPC SUV with Triton X-100 (0.5% w/v). Error bars indicate the SEM for quadruplicate determinations.

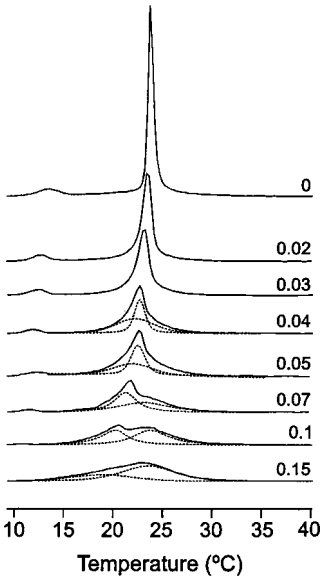

FIGURE 3: DSC heating thermograms of aqueous dispersions of DMPC (MLV) with the Bcl-2 C-terminal domain peptide obtained at different peptide/DMPC molar ratios as indicated. Components (- - -) were acquired by decomposition of the peaks and shown in the range of 0.04−0.15 peptide/DMPC molar ratios.

of the peptide in EYPC SUV model membranes, the release of encapsulated 5(6)-carboxyfluorescein trapped inside the vesicles was observed at increasing concentrations of peptide. Figure 2 shows percentages of release after 15 min of the addition of the peptide, illustrating how the peptide released 50% of the probe, at a peptide/lipid molar ratio of 0.06. This result indicates that the peptide may disrupt the barrier properties of the phospholipid bilayer by inserting itself into this membrane.

Differential Scanning Calorimetry. Multilamellar vesicles, of both pure DMPC and those containing different concentrations of the Bcl-2 C-terminal domain peptide, were studied by DSC with the aim of obtaining information on the way in which this peptide interacts with the membrane. Figure 3 shows that the presence of a low peptide content, as in a 0.02 peptide/DMPC molar ratio, only slightly increased the width of the main transition, while it broadened and decreased the onset of the pretransition peak by about 2 °C. At a 0.04 peptide/DMPC molar ratio, the pretransition was further shifted and the size of the peak further decreased and widened. This thermogram and those obtained at higher peptide concentrations were decomposed, and two components were observed. At a 0.04 peptide/DMPC molar ratio, a broad component was centered at about the same temperature as another narrower component, the last one having a bigger area as seen in Figure 4B. At a 0.05 peptide/lipid molar ratio, the transition peak was widened further, and its decomposition showed an increase of the broader component at the expense of the narrower one, both of them being of similar size. At a 0.07 peptide/DMPC molar ratio, a very clear shoulder appeared at the top edge, with the pretransition peak being very much reduced in size. The decomposition of this peak indicated that the area of the broad component has increased slightly although both components still maintain similar size. In addition to that, the maxima of both components have shifted. Thus, the broader component observed at 0.04 and 0.05 peptide/DMPC molar ratios at 21.3 °C has now shifted to 23.6 °C, probably corresponding to a phase rich in peptide. The narrower component observed at a lower peptide/lipid molar ratio has now shifted to 21.3 °C, probably corresponding to a phase with a lower content in peptide. At a 0.1 peptide/DMPC molar ratio, the pretransition peak was not detected, and two components appeared clearly separated. After decomposition of this peak, it was evident that both components were now wider and centered at 20.2 and 23.8 °C; the one centered at the higher temperature was bigger in size. Finally, at a 0.15 peptide/DMPC molar ratio, the decomposition of this peak showed that one of the components was much bigger and centered at 23.5 °C, whereas the smaller one was centered at 18.9 °C. The small size of this last peak probably indicated that the peptide concentration was so high that this phase with low content

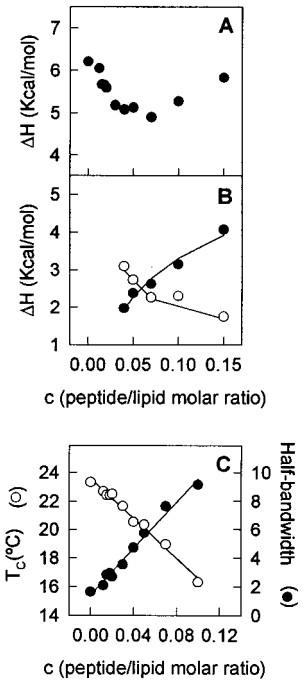

FIGURE 4: Data obtained from DSC thermograms of aqueous dispersions of DMPC (MLV) with the Bcl-2 C-terminal domain peptide shown in Figure 3. (A) Enthalpy change associated with the main gel−fluid phase transition. (B) Enthalpy changes associated with the components observed after decomposition of the main transition peaks with a lower transition temperature (○) and a higher transition temperature (●). (C) Dependence of the onset of temperature transition, T_C (○), and half-bandwidth (●) of the main transition peaks. Data were derived from thermograms in Figure 3 as described (*80*).

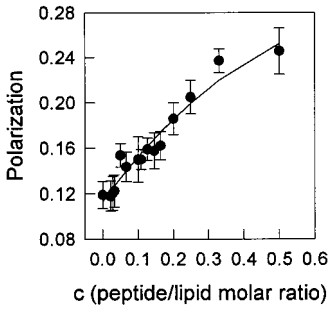

FIGURE 5: Polarization of DPH fluorescence in EYPC (MLV) (10 μM) (probe/lipid molar ratio of 1:500) with the Bcl-2 C-terminal domain at increasing molar fractions. Experiments were carried out at 25 °C and constant stirring. Measurements were made in two independent experiments with nine determinations for each experiment.

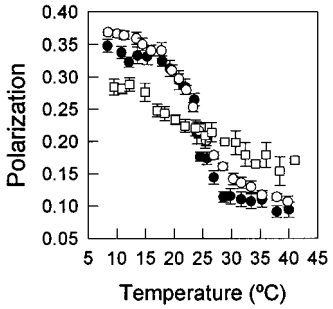

FIGURE 6: Fluorescence polarization as a function of temperature of DPH in DMPC (MLV) (probe/lipid molar ratio of 1:500) in the absence (●) or in the presence of the Bcl-2 C-terminal domain at 0.04 (○) and 0.5 (□) peptide/DMPC molar ratios. Experiments were carried out at constant stirring. Two independent experiments were carried out with nine determinations for each experiment.

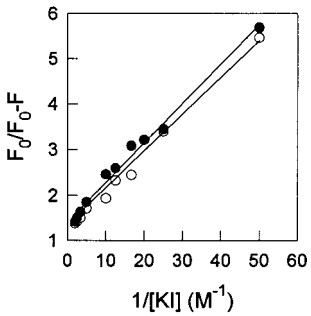

FIGURE 7: Modified Stern−Volmer plots of the quenching of tyrosine fluorescence of the Bcl-2 C-terminal domain peptide by KI. Peptide incorporated in EYPC (MLV) at a peptide/lipid molar ratio of 0.022 (●) and peptide alone (in the absence of phospholipid) (○) were assayed. Measurements were made in triplicate.

in peptide was very reduced. The appearance of a shoulder at the top edge of the main transition peak can be taken as an indication of peptide aggregation in the fluid state.

ΔH values for the transition peaks are shown in Figure 4A. It can be observed that there was a decrease in ΔH at low peptide concentrations (0−0.04 peptide/DMPC molar ratio), but no further decrease was observed at higher concentrations and even a certain recovery of ΔH values at 0.1 and 0.15 peptide/DMPC molar ratios. This pattern is most probably due to the aggregation of the peptide, as discussed above. The distribution of ΔH values corresponding to each of the two components obtained by decomposition of the transition peak in the range 0.04−0.15 peptide/DMPC molar ratios are depicted in Figure 4B. It can be seen how the peptide-rich component (broad) increases at the expense of the lipid component (narrow).

Figure 4C shows how the decrease in the onset temperature of the transition was accompanied by an increase in the half-bandwidth of the transition.

Fluorescence Probe Polarization Spectroscopy. With the aim of obtaining more information on the interaction of the Bcl-2 C-terminal domain peptide with membranes, experiments based on changes in fluorescence polarization of the probe DPH were carried out. Steady-state fluorescence polarization provides a time-averaged indication of the mobility of a fluorophore. DPH is a hydrophobic fluorescent molecule that, when incorporated into a lipid bilayer, is located in the hydrophobic region. In pure lipid bilayers, DPH is freely mobile, and its fluorescence is minimally polarized. The polarization of diphenylhexatriene fluorescence has been studied to understand protein-induced changes in lipid dynamics (*71*, *72*). The presence of intrinsic molecules, such as the peptide studied here, may hinder the motion of the fluorescent probe, thus increasing its polarization. Figure 5 depicts our studies made with a fluid membrane, as is the case with EYPC at 25 °C, and how increasing concentrations of the peptide produced increasing polarization values. These results are in agreement with the effects reported for other intrinsic molecules, such as Ca^{2+}-ATPase (*71*), cholesterol and cytochrome *c* oxidase (*73*), bacteriorhodopsin (*74*), myelin apolipoprotein (*75*), Pf-1 viral protein (*76*), and α-hemolysin (*72*).

DPH fluorescence polarization was also studied at different temperatures to monitor the influence of the Bcl-2 C-terminal domain peptide on the phase transition of DMPC vesicles in which it was incorporated (Figure 6). Concentration of the 0.04 peptide/lipid molar ratio did not result in any considerable broadening of the phase transition of pure phospholipid. However, at a 0.1 peptide/lipid molar ratio, the phase transition was so broadened that it was almost undiscernible. This means that polarization decreased below the phase transition but increased above the phase transition, indicating that an intermediate degree of apparent order is produced by the peptide, as a consequence of its interaction with the lipid acyl chains.

Quenching of the Intrinsic Fluorescence of the Bcl-2 C-Terminal Domain Peptide. To investigate the accessibility of the Tyr-235 residue to the aqueous solvent, experiments were carried out in which the fluorescence of this residue was quenched by increasing concentrations of KI. Figure 7 shows a modified Stern−Volmer plot, from which the K_Q values for the peptide in water without lipid and the peptide incorporated in EYPC vesicles were found to be 16.8 and 16.2 M^{-1}, respectively. Thus, both values are high and similar, meaning that the Tyr-235 residue is highly accessible to the aqueous solvent, even when the peptide is incorporated into phospholipid vesicles.

DISCUSSION

It has been suggested that the C-terminal hydrophobic domain of the Bcl-2 plays an important role in the subcellular localization of this protein. Given its very hydrophobic character, it is assumed that it serves as a membrane anchor. In addition, its insertion in membranes has been suggested by the fact that its elimination prevents the localization of Bcl-2 in cell membranes, such as mitochondria or endoplas-

mic reticulum (*26*−*29*). However, the structure and the interaction of this C-terminal domain of Bcl-2 with membranes have not previously been experimentally demonstrated. This paper is the first experimental study in which it has been shown that the C-terminal domain of Bcl-2 may insert itself in membranes where, in the presence of lipids, it adopts a predominantly α-helical structure.

The highly hydrophobic nature of the C-terminal domain, and hence of the 23mer peptide used in this paper to imitate its sequence, may explain why it self-aggregates in aqueous solvent in the absence of lipids, hence giving an infrared spectrum with a maximum at 1623 cm^{-1}. However, in the presence of phospholipid model membranes it dissociates, so that the 1623 cm^{-1} component becomes very small (6%) and the α-helical structure becomes the predominant one. Computer predictions made from the amino acid sequence also suggest that the α-helix would be the predominant structure (87%).

Insertion of the peptide in the model membranes was confirmed by the other experiments shown in this paper. Carboxyfluorescein leakage induced by the C-terminal domain of Bcl-2 indicates that this peptide penetrates the lipid hydrophobic core, breaking the barrier properties of the membrane, although it is not clear whether this effect is related to the physiological effect of Bcl-2 on the biological membranes. This protein has been shown to form a channel in mitochondrial membranes, but due to the insertion of helices α5 and α6 (*6*−*13*) and not to the C-terminal hydrophobic stretch which was chopped from the fragments used in the works mentioned. Nevertheless, it should be pointed out that the Bcl-2 inserted into the membrane may not only alter its permeability but also interact with specific proteins such as bap31 and BI-1 which are also located in the membrane of the endoplasmic reticulum (*77*).

Since the leakage of carboxyfluorescein was concentration dependent, it is interesting to discuss this in terms of the possible formation of a pore. It can be seen that the increase in leakage with peptide concentration was parallel to the increase of the broad component observed upon decomposition of DSC peaks and attributed to a peptide-rich phase (Figures 3 and 4B), and therefore it is tempting to speculate that the leakage takes place mainly through the regions of the membrane with high peptide contents where the association of peptide molecules may be facilitated.

DSC results pointed to a broadening of the main phase transition peak of DMPC with increasing concentrations of the peptide and, at the same time, a decrease in the pretransition peak, which finally disappeared at the 0.1 peptide/lipid molar ratio, behavior which can be expected from an intrinsic membrane protein (*78*). Also, the increase in fluorescence polarization of DPH produced by increasing concentrations of peptide strongly suggested that the peptide was inserted in the membrane as an intrinsic molecule. DPH is known to be freely mobile and its fluorescence to be minimally polarized, but the presence of intrinsic membrane proteins provides a time-averaged indication of the mobility of the fluorophore, increasing the apparent order of the membrane by restricting the mobility of the probe molecules. This effect is the same as that found for many other intrinsic molecules (*71*−*76*).

Study of the phase transition of DMPC both in the absence and in the presence of peptide by fluorescence polarization of DPH confirmed the results detected by DSC, namely, that the peptide produced a widening of the phase transition. In addition, it was found that the peptide decreased the polarization values of DPH at temperatures above the phase transition but increased these values below the phase transition. This again suggests that the peptide is an intrinsic molecule which behaves like other intrinsic molecules, such as cholesterol or gramicidin (*71*, *78*).

The fact that the intrinsic fluorescence of the Tyr residue of the peptide was quenched to a similar extent when incorporated into the membrane and when in solution indicates that this residue is located superficially in the membrane. This residue is the fifth from the N-terminus, so that the part protruding from the membrane probably ends with Leu-236, which is the residue following Tyr-235, since it has been predicted that the α-helical part ends precisely at this Leu-236 residue. This is in agreement with data which suggest the integral membrane nature of this domain and its cytoplasmic orientation when inserted in cellular membranes, such as the outer mitochondrial membranes (*26*, *27*).

It is necessary to emphasize here that different types of lipids have been used in the experiments discussed above. In this paper, FT-IR experiments, carboxyfluorescein leakage, the dependence of DPH fluorescence polarization on peptide/lipid ratio, and tyrosine fluorescence quenching were carried out with egg yolk phosphatidylcholine. However, in experiments in which the dependence with temperature was studied, such as DSC and DPH polarization, DMPC was used. The reason for that was that it was intended to use a phospholipid which is fluid at usual laboratory temperature like egg yolk phosphatidylcholine but to use DMPC in those experiments in which a cooperative phase transition was necessary. In addition to that, there were some variations in the peptide to lipid molar ratios in the different experimental techniques, as summarized below: it was 0.1 in FT-IR; 0−0.2 in the carboxyfluorescein leakage assay; 0−0.15 in DSC measurements; 0−0.5 in DPH fluorescence polarization at increasing molar fractions; 0, 0.04, and 0.5 in the fluorescence polarization of DPH as a function of temperature; and 0.02 in quenching of Tyr by iodide. These different ratios were chosen in order to clearly show the effects of peptide on lipid in all the experiments, and it should be remembered that the sensitivity of these techniques is not the same, and hence it is necessary to use different amounts of sample. Nevertheless, the use of different concentrations of peptide may cause some differential effects on the conformation, orientation, and aggregation state of the peptide segment in the lipid environment, and therefore some cautions are necessary when comparing the results obtained. Finally, whereas multibilayer vesicles were generally used, in the case of the release of carboxyfluorescein it was necessary to use unilamellar vesicles in order to have a system which may allow the observation of a simple kinetics of release.

Since the hydrophobic C-terminal domain studied here tends to aggregate, it is clear that it could not exist in a free state exposed to water in Bcl-2 molecules which are not integrated in cell membranes, which is in accordance with results demonstrating that Bcl-2 is posttranslationally integrated into membranes by means of this hydrophobic C-terminal domain (*27*, *79*).

In summary, our results experimentally show that the C-terminal domain of Bcl-2 adopts a predominantly α-helical

structure when inserted in membranes, where it behaves as an intrinsic molecule, altering the physical properties of the phospholipid bilayer. It would be extremely interesting to obtain at some future date enough full-length Bcl-2 protein to carry out structural studies such as those described here.

REFERENCES

1. Tsujimoto, Y., Cossman, J., Jaffe, E., and Croce, C. M. (1985) *Science 228*, 1440−1443.
2. Kroemer, G. (1997) *Nat. Med. 3*, 614−620.
3. Chao, D. T., and Korsmeyer, S. T. (1998) *Annu. Rev. Immunol. 16*, 395−419.
4. Yin, X. M., Oltvail, Z. N., and Korsmeyer, S. J. (1994) *Nature 369*, 321−323.
5. Reed, J. C. (1994) *J. Cell Biol. 124*, 1−6.
6. Yang, J., Liu, X., Bhalla, K., Kim, C. N., Ibrado, A. M., Cai, J., Peng, T. I., Jones, D. P., and Wang, X. (1997) *Science 275*, 1129−1132.
7. Kluck, R. M., Bossy-Wetzel, E., Green, D. R., and Newmeyer, D. D. (1997) *Science 275*, 1132−1136.
8. Antosson, B., Conti, F., Ciavatta, A. M., Montessuit, S., Lewis, S., Martinou, I., Bernasconi, L., Bernard, A., Mermod, J. J., Mazzei, G., Maundrell, K., Gambasale, F., Sadoul, R., and Martinou, J. C. (1997) *Science 277*, 370−372.
9. Minn, A. J., Vélez, P., Schendel, S. L., Liang, H., Muchmore, S. W., Fesik, S. W., Fill, M., and Thompson, C. B. (1997) *Nature 385*, 353−357.
10. Schlensiger, P. H., Gross, A., Yin, X. M., Yamamoto, K., Saito, M., Waksman, G., and Korsmeyer, S. J. (1997) *Proc. Natl. Acad. Sci. U.S.A. 94*, 11357−11362.
11. Van der Heiden, M. G., Chandel, N. S., Williamson, E. K., Schumacker, P. T., and Thompson, C. B. (1997) *Cell 91*, 627−637.
12. Schendel, S. L., Xie, Z., Montal, M. O., Matsuyama, S., Montal, M., and Reed, J. C. (1997) *Proc. Natl. Acad. Sci. U.S.A. 94*, 5113−5118.
13. Shimizu, S., Eguchi, Y., Kamiike, W., Funahashi, Y., Mignon, A., Lacronique, V., Matsuda, H., and Tsujimoto, Y. (1998) *Proc. Natl. Acad. Sci. U.S.A. 95*, 1455−1459.
14. Rossé, T., Olivier, R., Monney, L., Rager, M., Conus, S., Fellay, I., Jansen, B., and Borner, C. (1998) *Nature 391*, 496−499.
15. Narita, M., Shimizu, S., Ito, T., Cittenden, T., Lutz, R. J., Matsuda, H., and Tsujimoto, Y. (1998) *Proc. Natl. Acad. Sci. U.S.A. 95*, 14681−14687.
16. Shimizu, S., Narita, M., and Tsujimoto, Y. (1999) *Nature 399*, 483−487.
17. Jans, D. A., Sutton, V. R., Jans, P., Froelich, C. J., and Trapani, J. A. (1999) *J. Biol. Chem. 274*, 3953−3961.
18. Reed, J. C. (1997) *Nature 387*, 773−776.
19. Oltvai, Z. N., and Korsmeyer, S. J. (1994) *Cell 79*, 189−192.
20. Green, D. R., and Reed, J. C. (1998) *Science 281*, 1309−1312.
21. Fernandez-Sarabia, M. J., and Bischoff, J. R. (1993) *Nature 366*, 274−275.
22. Wang, H. G., Rapp, U. R., and Reed, J. C. (1996) *Cell 87*, 629−638.
23. Shibasaki, F., Kondo, E., Agaki, T., and McKeon, F. (1997) *Nature 386*, 728−731.
24. Naumovski, L., and Cleary, M. L. (1996) *Mol. Cell. Biol. 16*, 3884−3892.
25. Froesch, B. A., Aimé-Sempé, C., Leber, B., Andrews, D., and Reed, J. C. (1999) *J. Biol. Chem. 274*, 6469−6475.
26. Chen-Levy, S., Nourse, J., and Cleary, M. L. (1989) *Mol. Cell. Biol. 9*, 701−710.
27. Nguyen, M., Millar, D. G., Yong, V. W., Korsmeyer, S. J., and Shore, G. C. (1993) *J. Biol. Chem. 268*, 25265−25268.
28. Krajewski, S., Tanaka, S., Takayama, S., Schibler, M. J., Fenton, W., and Reed, J. C. (1993) *Cancer Res. 53*, 4701−4714.
29. Akao, Y., Otsuki, Y., Kataoka, S., and Tsujimoto, Y. (1994) *Cancer Res. 54*, 2468−2471.
30. Hockenbery, D. M., Oltvai, Z. N., Yin, X. M., Milliman, C. L., and Korsmeyer, S. J. (1993) *Cell 75*, 241−251.
31. Nguyen, M., Branton, P. E., Walton, P. A., Oltvai, Z. N., Korsmeyer, S. J., and Shore, G. C. (1994) *J. Biol. Chem. 269*, 16521−16524.
32. Tanaka, S., Saito, K., and Reed, J. C. (1993) *J. Biol. Chem. 268*, 10920−10926.
33. Borner, C., Martinou, I., Mattmann, C., Scaerer, E., Martinou, J. C., and Tschopp, J. (1994) *J. Cell Biol. 126*, 1059−1068.
34. Vance, B. A., Zacharchuk, C. M., and Segal, D. M. (1996) *J. Biol. Chem. 48*, 30811−30815.
35. Schlesinger, P. L., Gross, A., Yin, X. M., Yamamoto, K., Saito, M., Waksman, and Korsmeyer, S. J. (1997) *Proc. Natl. Acad. Sci. U.S.A. 94*, 11357−113632.
36. Narita, M., Shimizu, S., Ito, T., Chittenden, T., Lutz, R. J., Matsuda, H., and Tsujimoto, Y. (1998) *Proc. Natl. Acad. Sci. U.S.A. 95*, 14681−14686.
37. Basañez, G., Nechustan, A., Drozhinin, O., Chanturiya, A., Choe, E., Tutt, S., Wood, K. A., Hsu, Y. T., Zimmemberg, J., and Youle, R. J. (1999) *Proc. Natl. Acad. Sci. U.S.A. 96*, 5492−5497.
38. Muchmore, S. W., Sattler, M., Liang, H., Meadows, R. P., Harlan, J. E., Yoon, H. S., Nettesheim, D., Chang, B. S., Thompson, C. B., Wong, S. L., Ng, S. C., and Fesik, S. W. (1996) *Nature 381*, 335−341.
39. Aritomi, M., Kunishima, N., Inohara, N., Ishibashi, Y., Ohta, S., and Morikawa, K. (1997) *J. Biol. Chem. 272*, 27886−27892.
40. Rost, B., and Sander, C. (1993) *J. Mol. Biol. 232*, 584−599.
41. Rost, B., and Sander, C. (1994) *Proteins 19*, 55−72.
42. Arrondo, J. L. R., Muga, A., Castresana, J., Valpuesta, J. M., and Goñi, F. M. (1989) *FEBS Lett. 252*, 118−120.
43. Arrondo, J. L. R., Castresana, J., Valpuesta, J. M., and Goñi, F. M. (1994) *Biochemistry 33*, 11650−11655.
44. Schägger, H., and Von Jagow, G. (1987) *Anal. Biochem. 166*, 368−379.
45. Lehrer, S. S., and Leavis, P. C. (1978) *Methods Enzymol. 49*, 222−236.
46. Lakowicz (1983) in *Principles of fluorescence spectroscopy*, pp 112−152, Plenum Press, New York and London.
47. Böttcher, C. S. F., Van Gent, C. M., and Fries, C. (1961) *Anal. Chim. Acta 24*, 203−204.
48. Weinstein, J. N., Yoshikami, S., Henkart, P., Blumenthal, R., and Hagins, W. A. (1977) *Science 195*, 489−492.
49. Rex, S. (1996) *Biophys. Chem. 58*, 75−85.
50. Rex, S., and Schwarz, G. (1998) *Biochemistry 37*, 2336−2345.
51. Simon, C. G., and Gear, A. R. L. (1998) *Biochemistry 37*, 2059−2069.
52. Ralston, E., Hjelmeland, L. M., Klausner, R. D., Weinstein, J. N., and Blumenthal, R. (1981) *Biochim. Biophys. Acta 649*, 133−137.
53. Clark, A., Saunderson, D., and Sugget, A. (1981) *Int. J. Pept. Protein Res. 17*, 353−364.
54. Arrondo, J. L. R., Young, N. M., and Manstch, H. H. (1988) *Biochim. Biophys. Acta 952*, 261−268.
55. Haltia, T., Semo, N., Arrondo, J. L. R., Goñi, F. M., and Freire, E. (1994) *Biochemistry 33*, 9731−9740.
56. García-García, J., Corbalán-García, M. S., and Gómez-Fernández, J. C. (1999) *Biochemistry 38*, 9667−9675.
57. Arrondo, J. L. R., Muga, A., Castresana, J., and Goñi, F. M. (1993) *Prog. Biophys. Mol. Biol. 59*, 23−56.
58. Arrondo, J. L. R., and Goñi, F. M. (1999) *Prog. Biophys. Mol. Biol. 72*, 367−405.
59. Krim, S., and Bandekar, J. (1986) *Adv. Protein Chem. 38*, 181−364.
60. Susi, H., and Byler, D. M. (1987) *Arch. Biochem. Biophys. 258*, 465−469.
61. Fabian, H., Naumann, D., Misselwitz, R., Ristau, O., Gerlach, D., and Welfle, H. (1992) *Biochemistry 31*, 6532−6538.
62. Gonzalez, M., Bagatolli, L. A., Echabe, I., Arrondo, J. L. R., Argaraña, C. E., Cantor, C. R., and Fidelio, G. D. (1997) *J. Biol. Chem. 272*, 11288−11294.
63. Zhang, H., Ishikawa, Y., Yamamoto, and Carpentier, R. (1998) *FEBS Lett. 426*, 347−351.

64. Surewicz, W. K., Leddy, J. J., and Mantsch, H. H. (1990) *Biochemistry 29*, 8106−8111.
65. Fabian, H., Schultz, C., Naumann, D., Landt, O., Hahn, and Saenger, W. (1993) *J. Mol. Biol. 232*, 967−981.
66. Muga, A., Arrondo, J. L. R., Bellon, T., Sancho, J., and Bernabeu, C. (1993) *Arch. Biochem. Biophys. 300*, 451−457.
67. Azuaga, A. I., Sepulcre, F., Padrós, E., and Mateo, P. L. (1996) *Biochemistry 35*, 16328−16335.
68. Chehin, R., Iloro, I., Marcos, M. J., Villar, E., Shnyrov, V. L., and Arrondo, J. L. R. (1999) *Biochemistry 38*, 1525−1530.
69. Quinn, P. J., and Chapman, D. (1980) *CRC Crit. Rev. Biochem. 8*, 1−117.
70. Susi, H., Timashef, S. N., and Stevens, L. (1967) *J. Biol. Chem. 242*, 5460−5466.
71. Gómez-Fernández, J. C., Goñi, F. M., Bach, D., Restall, C. J., and Chapman, D. J. (1980) *Biochim. Biophys. Acta 598*, 502−516.
72. Soloaga, A., Veiga, M. P., García-Segura, L. M., Ostolaza, H., Brasseur, R., and Goñi, F. M. (1999) *Mol. Microbiol. 31*, 1013−1024.
73. Hoffmann, W., Pink, D. A., Restall, C. J., and Chapman, D. (1981) *Eur. J. Biochem. 114*, 114−585.
74. Alonso, A., Restall, C. J., Turner, M., Gómez-Fernández, J. C., Goñi, F. M., and Chapman, D. (1982) *Biochim. Biophys. Acta 689*, 283−289.
75. Goñi, F. M., Cózar, M., Alonso, A., Durrani, A., García-Segura, L. M., Lee, D., Monreal, J., and Chapman, D. (1988) *Eur. J. Biochem. 174*, 641−646.
76. Azpiazu, I., Gómez-Fernández, J. C., and Chapman, D. (1993) *Biochemistry 32*, 10720−10726.
77. Ng, F. W. H., and Shore, G. C. (1998) *J. Biol. Chem. 273*, 3140−3143.
78. Chapman, D., Gómez-Fernández, J. C., and Goñi, F. M. (1979) *FEBS Lett. 98*, 211−223.
79. Chen-Levy, Z., and Cleary, M. L. (1990) *J. Biol. Chem. 265*, 2929−4923.
80. Eliasz, A. W., Chapman, D., and Ewing, D. F. (1976) *Biochim. Biophys. Acta 448*, 220−230.

BI000256H